

¹Jing Su
²Caiguang Liu
³Rong Zhang
⁴Zhenlin Wang
^{5,*}Yingyao Qin
⁶Gong Zhang

A Joint Inversion Method Algorithm for T2-Pc two Dimensional NMR based on Logistic Functions



Abstract: - Data processing is a key step in the analysis of nuclear magnetic resonance (NMR) experimental data, and efficient and accurate computer inversion algorithms are the core of the T2-Pc two-dimensional NMR experiment. T2-Pc two-dimensional NMR experiment is an advanced experimental method that characterizes reservoir connectivity through two dimensions: relaxation time and capillary pressure, and can obtain irreducible water saturation under different pressure differences. However, the algorithm currently used for T2-Pc two-dimensional spectrum inversion uses a mutation kernel function, resulting in low accuracy of calculation results. This paper uses the Logistic function as the two-dimensional inversion kernel function, rewrites the inversion algorithm, and obtains more accurate inversion results. Numerical simulations have proven that the T2-Pc two-dimensional map obtained by this method not only has higher resolution, but also has greater applicability in the case of low signal-to-noise ratio and a small number of centrifugal echo groups. Practice has found that the proposed method can reduce the number of centrifugations during the experiment and significantly improve the efficiency of T2-Pc two-dimensional nuclear magnetic resonance experiments.

Keywords: Data process algorithm, Nuclear magnetic resonance, Inversion algorithm, Logistic function, Connectivity, Relaxation, Capillary pressure.

I. INTRODUCTION

Nuclear magnetic resonance (NMR) technology can observe the relaxation characteristics of fluids in porous media such as cores and is widely used in well logging and laboratory core analysis [1-3]. The spin-spin relaxation time T2 measured by nuclear magnetic resonance experiment can reflect the size distribution characteristics of rock pores. The NMR experiment calibration of core samples in the laboratory can characterize the movable fluid and accurately estimate the saturation of the irreducible fluid in the downhole reservoir [4-6]. The T2 cutoff value is determined by measuring the core samples in saturated and centrifugally dehydrated states, and the irreducible water saturation can be obtained. This has become a standard petrophysical analysis method [7-9]. The irreducible water saturation is an important parameter that determines the development effect of low permeability oil and gas reservoirs and is also a key indicator of reservoir productivity evaluation [10-11].

In standard NMR core analysis experiments, the centrifugal force required for different reservoir samples is different. In order to obtain accurate irreducible water saturation, how to select the appropriate centrifugal force in the centrifugal experiment has become a difficult problem [12-14]. To address this problem, centrifugal experiments were carried out on carbonate rock, tight sandstone, and shale reservoirs to determine the optimal centrifugal force combined centrifugal experiments and NMR measurements to obtain the NMR T2 distribution and fluid saturation variation characteristics of tight reservoirs in the Ordos Basin under different centrifugal forces [15-20]. Zhang et al. obtained the lower limit of the pore throat of the movable fluid distribution through NMR and multiple centrifugation experiments [21]. It was also verified using methods such as capillary pressure curves, showing that multiple centrifugal pressures NMR experiments can obtain lower limits of physical properties and thus evaluate reservoir effectiveness. Jiang et al. measured the T2 distribution of multiple centrifugations of tight sandstone and estimated the core surface relaxation rate based on multiple T2 cutoff values [22]. Li et al. used Bayesian optimisation with transfer learning to study NMR surface relaxation rates [23]. Thereby they characterized the pore size distribution from the surface relaxation rate. Elsayed et al. used the Hassler-Brunner equation to convert the rotational speed of the centrifugal experiment into capillary pressure data

¹ Exploration and Development Research Institute of PetroChina Xinjiang Oilfield Company, Xinjiang, China

² Exploration and Development Research Institute of PetroChina Xinjiang Oilfield Company, Xinjiang, China

³ Exploration and Development Research Institute of PetroChina Xinjiang Oilfield Company, Xinjiang, China

⁴ Exploration and Development Research Institute of PetroChina Xinjiang Oilfield Company, Xinjiang, China

⁵ MRT&A Magnetic Resonance Technology and Application Laboratory, Yangtze University, Wuhan, Hubei, China

⁶ MRT&A Magnetic Resonance Technology and Application Laboratory, Yangtze University, Wuhan, Hubei, China

*Corresponding author: Yingyao Qin

Copyright © JES 2024 on-line : journal.esrgroups.org

to calculate the USBM (U.S. Bureau of Mines, Texas) wettability index and study the wettability change of the reservoir [24-25].

The capillary pressure can be obtained from the data of multiple centrifugal experiments, which indicates the connectivity of the reservoir [26]. However, multiple centrifugal experiments have heavy workloads and difficulties in data processing and analysis. Chen et al. proposed the T2-Pc (Pc is capillary pressure) core testing technology [27]. The T2-Pc maps were obtained using the NMR experimental data obtained under different centrifugal force conditions and processed by T2 distribution domain difference (T2SDD) or differential echo inversion (DEI) methods. It makes up for the inadequacy of conventional saturated and centrifugal NMR experiments that cannot reflect connectivity. The irreducible fluid saturation can be obtained from the T2-Pc distribution at any production pressure differential. Based on the development of 2D NMR technology and the idea of multi-dimensional magnetic resonance (MR) spectroscopy [28-31], Song et al. conduct relevant research on different physical processes [32]. He introduced non-MR physical quantities in the NMR dimension for 2D NMR inversion. For the NMR experimental data under different centrifugal force conditions, he proposed a joint inversion algorithm of multiple groups of echoes to directly obtain the 2D correlation distribution of relaxation time (T2) and capillary pressure (Pc). This method not only solves the disadvantage of the T2SDD algorithm that is prone to negative values, but also solves the cumbersome problem of data processing in the DEI algorithm, and is currently the best T2-Pc 2D NMR data processing algorithm. In practice, it was found that the data processed using Song's proposed joint echo inversion algorithm (JEI) has the phenomenon of abrupt changes in the Pc dimension. As shown in Fig. 1, there are sudden changes of data in the part indicated by the arrow in the figure, which cannot truly reflect the continuous changes of capillary pressure corresponding to different pores. This problem is more serious when the number of experimental centrifugal force groups is small.

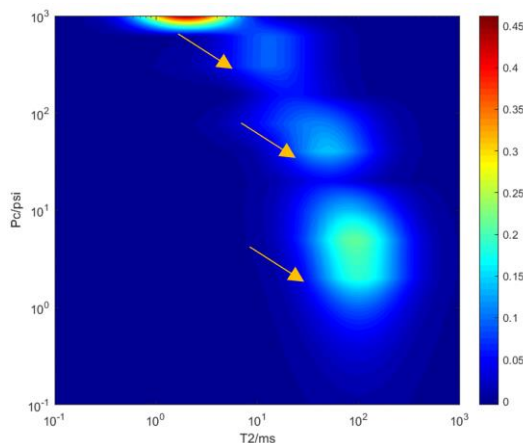


Fig. 1: T2-Pc Map by Inversion of the JEI Method

This paper briefly describes the experimental method and data processing method of the multi-dimensional and multi-physics T2-Pc 2D NMR technique. A detailed analysis of the joint echo inversion algorithm (JEI) based on the Heaviside step function as the kernel function is presented, and it is proposed to use the continuously varying logistic function as the kernel function for improvement. The Logistic function is helpful to improve the discontinuity of T2-Pc distribution. The joint inversion method (JEI-L) of T2-Pc 2D NMR echoes based on the logistic function is obtained. In comparison to prior investigations, this study introduces an innovative T2-Pc 2D spectral inversion kernel function. This novel approach significantly reduces the time required to acquire T2-Pc 2D spectra, while yielding more precise results from experimental data with low SNR.

II. METHOD

A. Conventional Data Processing Methods

The commonly used data processing methods for T2-Pc 2D NMR core experiments include the T2 distribution domain difference method (T2SDD) and differential echo inversion method (DEI), both of which are T2-Pc maps established indirectly from capillary pressure (Pc) and NMR T2 distribution.

1) T2SDD

After the water-saturated core is displaced by the centrifugal force of different magnitudes, the echo signals measured by the NMR experiment are inverted to obtain multiple T2 distribution. The T2 distribution of two adjacent centrifugal forces of different sizes are subtracted according to Eq. (1). The T2 distribution corresponding to the movable fluid components displaced by different centrifugal forces were obtained. Then, the

T2 distribution corresponding to different centrifugal forces (capillary pressures) and the movable fluids displaced by them are projected into the two-dimensional space, and the T2-Pc two-dimensional distribution is established.

$$T_{2,n+1} = T_{2,Pc(n)} - T_{2,Pc(n+1)}, \quad n = 0,1,2, \dots, m \quad (1)$$

where $T_{2,n+1}$ is the T2 distribution for the (n+1)-th and nth centrifugal forces (Pc). $T_{2,Pc(n)}$ is the T2 distribution of the core after the nth centrifugal force. When $n = 0$, the core is in a saturated state.

2) *DEI*

The differential echo inversion method (DEI) is to process the echo signal measured by the experiment. According to the magnitude of the centrifugal force, the echo signals of the two groups of different centrifugal forces are sequentially differentiated according to Eq. (2) to obtain the echo signals of the movable fluid displaced by the different centrifugal forces. Then the differential echo signals are inverted respectively to obtain T2 distribution of different centrifugal forces. Finally, the T2-Pc map is established according to the centrifugal force (capillary pressure) and the T2 distribution.

$$ECHO_{n+1} = ECHO_{Pc(n)} - ECHO_{Pc(n+1)}, \quad n = 0,1,2, \dots, m \quad (2)$$

where $ECHO_{n+1}$ is the NMR echo signal corresponding to the displacement of the movable fluid component between the (n+1)-th and n-th centrifugal forces (Pc). $ECHO_{Pc(n)}$ is the NMR echo signal measured after the n-th centrifugal force. When $n = 0$, the core is in a saturated state.

B. *Joint Echo Inversion Method (JEI)*

T2-Pc 2D NMR experiments measured multiple groups of NMR echo signals under different centrifugal forces (capillary pressure, Pc). The T2-Pc map can be obtained by inverting multiple echo signals using the joint echo inversion method (JEI). The amplitude of the echo signal obtained from the T2-Pc 2D NMR experiment obeys the multi-exponential decay law with the measurement time [32].

$$b_{i,k} = \sum_{j=1}^m \sum_{r=1}^n f_{j,r} \cdot \exp(-t_i/T_{2j}) H(Pc_r - p_k) \quad (3)$$

where $b_{i,k}$ is the amplitude of the i-th echo at the k-th centrifugal force. T2 is the transverse relaxation time. Pc is the capillary pressure. $f_{j,r}$ is the fluid component signal with transverse relaxation time T_{2j} and capillary pressure Pc_r . $H(Pc_r - p_k)$ is the Heaviside step function, and p_k is the centrifugal force of the core experiment. Using the multi-echo train joint inversion method to invert Eq. (3) to obtain $f_{j,r}$, that is, the 2D distribution of T2-Pc. The inversion kernel function of the JEI method consists of two parts. $\exp(-t_i/T_{2j})$ is used to describe the transverse relaxation process of NMR signal decay with time. $H(Pc_r - p_k)$ is used to describe the process of fluid signal decay with the change of displacement force, as shown in Eq. (4).

$$H(Pc_r - p_k) = \begin{cases} 0, & Pc_r \leq p_k \\ 1, & Pc_r > p_k \end{cases} \quad (4)$$

The kernel function used to describe the transverse relaxation decay process conforms to the law of echo signal decay. However, the Heaviside step function used to describe the effect of centrifugal displacement force change on the fluid is a mutation function as shown in Fig. 2 [33-34].The physical implication is that when the centrifugal displacement force p_k is greater than the capillary pressure Pc_r that the fluid component needs to overcome to discharge the core pores, the fluid component completely drives away from the sample, and its NMR signal cannot be measured. Conversely, the fluid component is not displaced and its signal can still be measured.

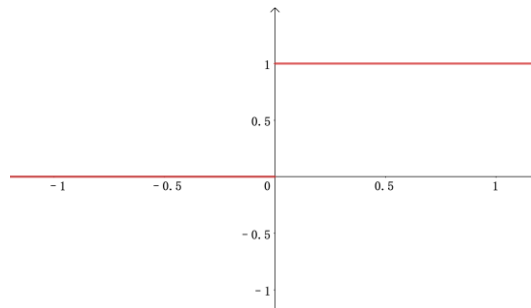


Fig. 2: Heaviside Step Functions

It should be noted that the inversion algorithm divides the fluid signal into n fluid types in the capillary pressure dimension. For the nth fluid type, the capillary pressure is not a point, but a neighborhood range ($Pc_n - \delta, Pc_n + \delta$). In contrast, in the centrifuge experimental data, the capillary pressure corresponding to each group of echoes is a certain value Pc_r , resulting in the mismatch between the experimental data and the inversion model.

In the $(Pc_n - \delta, Pc_n + \delta)$ domain, when Pc_r is equal to Pc_n , the n-th fluid type should be completely driven away from the sample according to the $H(Pc_r - p_k)$ kernel function of the JEI inversion method, so that the signal of the NMR measurement is 0. But the fact is that in this half of the $(Pc_n, Pc_n + \delta)$, the fluid is not completely driven away. Therefore, it is obviously inappropriate to directly use the Heaviside step function as the kernel function to describe the influence of the displacement force changes on the fluid NMR signal, which is likely to cause an abrupt change in the Pc dimension signal.

C. Joint Echo Inversion Method Based on the Logistic Function

There will be problems in using the mutation function as the kernel function, and it is necessary to use a suitable continuous function to optimize the inversion kernel function. As a common continuously variational shape function, the logistic function has a simple expression and can be used to describe the change of the NMR echo signal with the centrifugal displacement force [35,36]. Its expression is as shown in Eq. (5).

$$L(Pc_r - p_k) = \frac{1}{1 + \exp(-A(Pc_r - p_k))} \quad (5)$$

where Pc is the capillary pressure required for the fluid components to be driven away. p_k is the centrifugal force used in the experiment. A is a constant, and the larger A is, the faster the logistic function changes.

After replacing the Heaviside kernel function in the JEI inversion algorithm with the logistic function, an improved T2-Pc 2D NMR inversion algorithm (JEI-L) is obtained, and its expression is shown in Eq. (6).

$$b_{i,k} = \sum_{j=1}^m \sum_{r=1}^n f_{j,r} \cdot \exp(-t_i/T_{2j}) L(Pc_r - p_k) \quad (6)$$

where the improved kernel function describing the variation of the repulsion force is a logistic function. As shown in Fig. 3, for the fluid type n with capillary pressure Pc_n , $L(Pc_r - p_k) = 0.5$ is obtained when the centrifugal force p_k applied in the experiment is exactly equal to Pc_n . This indicates that only half of the fluid of this fluid type was displaced out of the sample, consistent with a gradual process of fluid displacement over a small neighborhood scale.

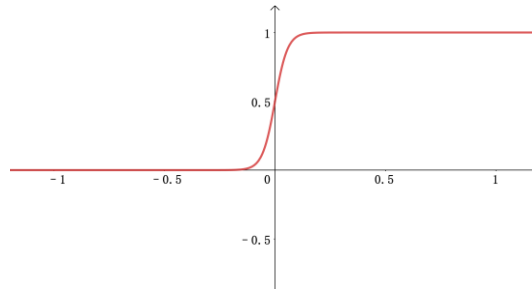


Fig. 3: Logistic Function

III. Numerical experimental and Result

A. Construction of T2-Pc Distribution

To verify the accuracy and applicability of the improved joint echo inversion method (JEI-L) in the T2-Pc 2D NMR core experiment, the numerical simulation method was used for verification. A 2D NMR distribution of T2-Pc with four components shown in Table 1 were was constructed according to the equation for the 2D Gaussian distribution [37] in double logarithmic coordinates shown in Eq. (7).

$$A_{i,j} = \sum_{g=1}^4 F_g \frac{1}{2\pi\sigma_{1g}\sigma_{2g}\sqrt{1-\rho_g^2}} \exp \left[-\frac{1}{2(1-\rho_g^2)} \left(\frac{(\ln T_{2i} - \ln T_{2g,mid})^2}{2\sigma_{1g}^2} + \frac{(\ln Pc_j - \ln Pc_{g,mid})^2}{2\sigma_{2g}^2} - \frac{2\rho_g(\ln T_{2i} - \ln T_{2g,mid})(\ln Pc_j - \ln Pc_{g,mid})}{\sigma_{1g}\sigma_{2g}} \right) \right] \quad (7)$$

where i (i=1, 2, 3, ..., m), j (j=1, 2, 3, ..., n) are the number of points in the constructed distribution. $A_{i,j}$ is the signal amplitude of each component. T_{2i} is the T_2 of the i-th column component. Pc_j is the capillary pressure corresponding to the j-th row component. F_g is the porosity component of the g-th pore. $T_{2g,mid}$ is the T2 relaxation center value of the g-th fluid. $T_{2g,mid}$ is the average value of the capillary pressure of the g-th fluid. σ_1 and σ_2 can control the spreading width of the distribution. ρ is the correlation coefficient of T_2 and Pc.

Fig. 4 shows the constructed T2-Pc two-dimensional distribution model, and the NMR echo signals under different displacement forces collected according to the model simulation. For the construction model, 15 groups

of echo signals of different centrifugal displacement pressures were simulated, and the pressure range was 0.12 psi~811 psi. The echo time (TE) of the simulated NMR echo signal acquisition is 0.4ms, the number of echoes (NECH) is 2000, and the waiting time (TW) is 10000ms. During simulations, each displacement pressure was set to displace the corresponding fluid components in the construction model.

Table 1: Details of the 4 Components of the Construction Model

Components	A	B	C	D
T_2	8	10	20	200
P_c	1000	100	10	1

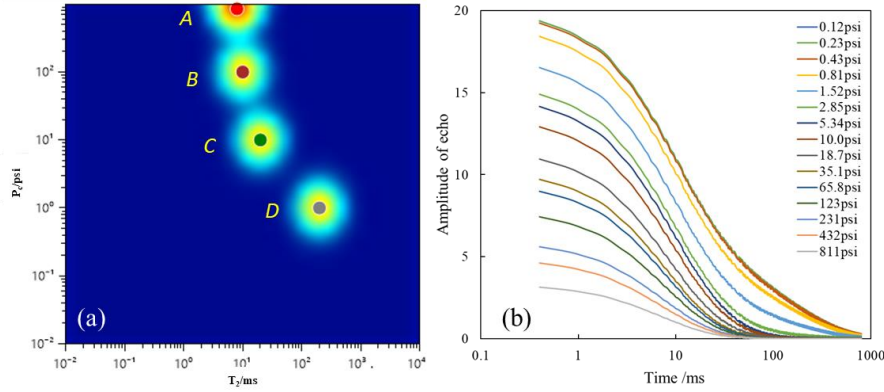


Fig. 4: Constructing the Model. (a) Constructing the T2-Pc Two-Dimensional Model; (b) Analog Acquisition Signals

B. Numerical Simulation Result

The JEI algorithm and the improved JEI-L algorithm were used to process the echo data of the T2-Pc 2D NMR experiment collected by simulation, and the results were shown in Fig. 5 and Fig. 7.

The results of T2-Pc distribution obtained using the two methods for 15 sets of centrifugal force echo data of different sizes with simulated SNRs of 100, 20, and 4 are shown in Fig.5. The inversion of T2 from 0.01-10000 points 64 steps, Pc from 0.01-1000 points 64 steps. Compared with the constructed model in Fig. 4(a), the T2-Pc map at SNR=100 is the closest to the model. As the SNR decreases, there was obvious noise on the left of the fluid signal in the T2-Pc maps, and the shape of the fluid signal changed, which was different from the model. Fig. 6 shows the Pc component information in the T2-Pc maps obtained by the two methods at different SNRs. The Pc component of JEI-L is closer to the construction model. In the case of lower SNR, the results obtained by the JEI-L method based on the logistic function can more clearly distinguish the fluid components of different Pc centrifugal forces and are relatively closer to the construction model.

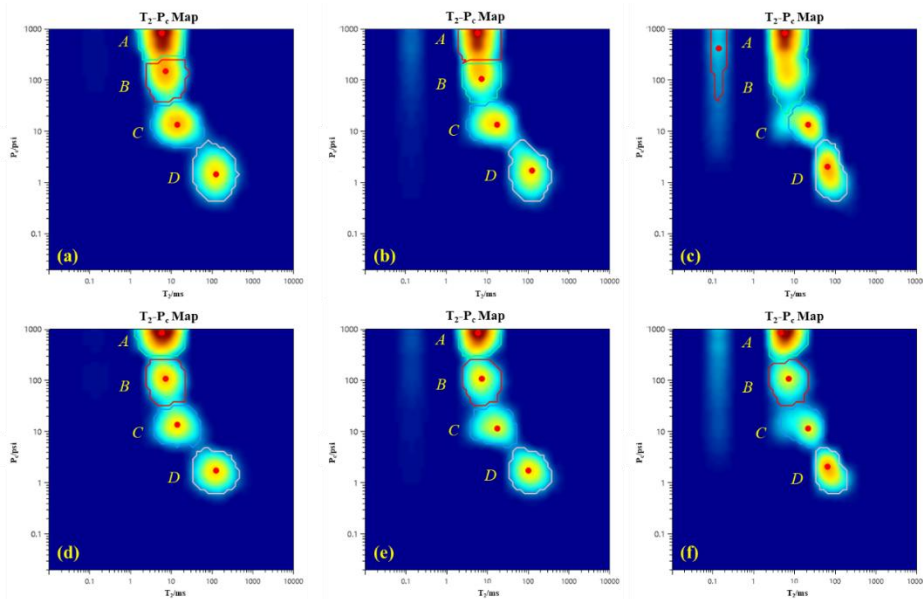


Fig. 5: Simulation of T2-Pc Distribution with Different SNR. (a) JEI Method and SNR=100; (b) JEI Method and SNR=20; (c) JEI Method and SNR=4; (d) JEI-L Method and SNR=100; (e) JEI-L Method and SNR=20; (F) JEI-L Method and SNR=4

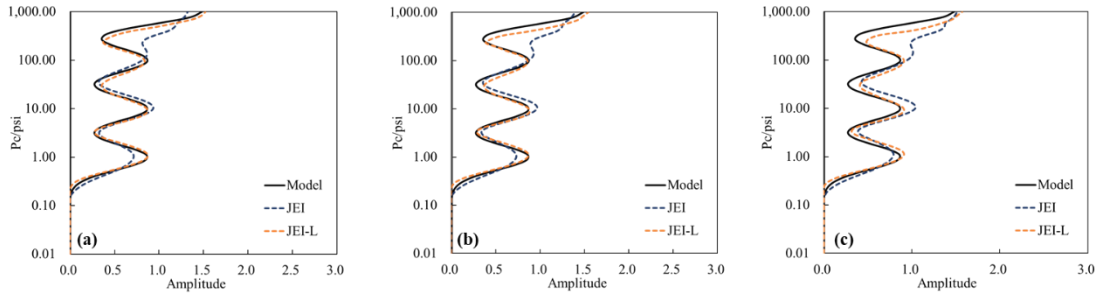


Fig.6: Pc Components of T2-Pc Maps with Different SNR. (a) SNR=100; (b) SNR=20; (c) SNR=4

In the case of signal-to-noise ratio SNR = 20, the echo data collected under different centrifugal force groups of 15,11 and 7 groups are simulated respectively. The T2-Pc distribution results obtained by the two methods are shown in Fig 7. Compared with the construction model in Fig. 4(a), the T2-Pc maps when the number of centrifugal force groups is 15 are the closest to the model. As the number of centrifugal force groups decreases, the boundaries of different fluid signals become blurred. It is difficult to distinguish the fluid components in the dimension of displacement force Pc. Fig. 8 shows the Pc component information in the T2-Pc maps obtained by the two methods when the number of centrifugal force groups is different, and the Pc component of JEI-L is closer to the structural model. In the case of reducing the number of centrifugal force groups, compared with the results of JEI, the boundary of the fluid signal of the T2-Pc maps inverted by the improved JEI-L method is more obvious and closer to the structural model, indicating that the improved JEI-L method has obvious advantages. The correlation coefficients (R2) were used to measure the relationship between the inversion results and the tectonic model, and the R2 between JEI and JEI-L and the tectonic model obtained from Fig. 6 and Fig.8 were shown in Table 2. The correlation coefficients of the JEI-L results were significantly higher than those of the JEI method.

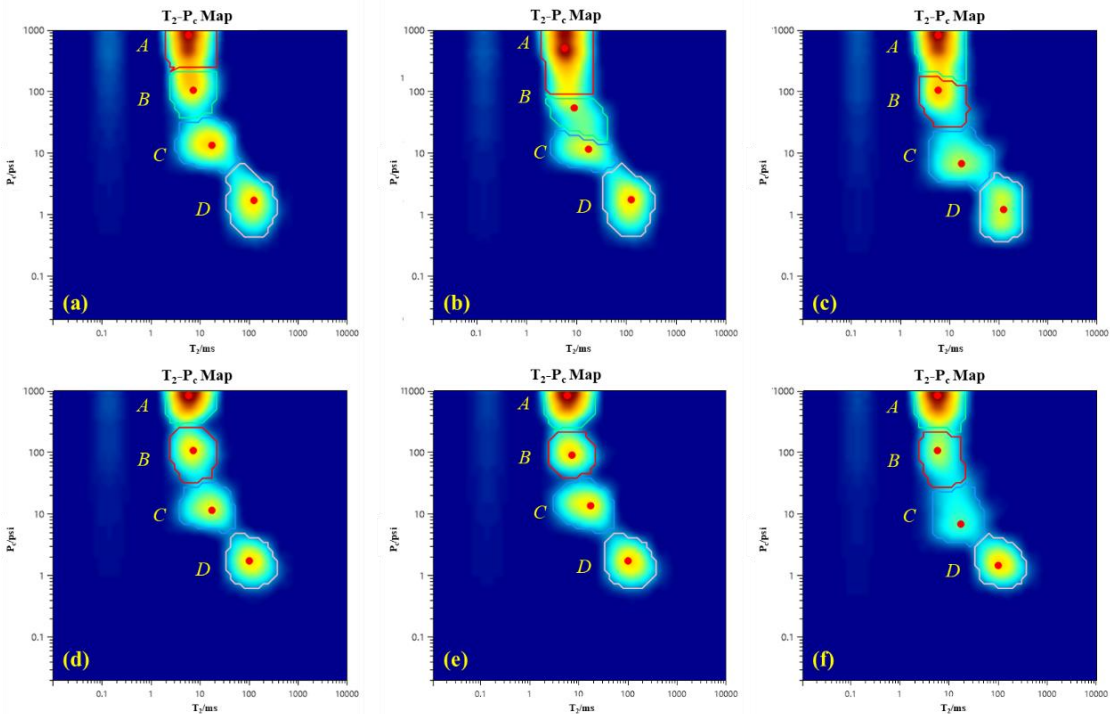


Fig. 7: Simulation of T2-Pc Distribution for Different Centrifugal Forces. (a) JEI Method and Groups=15; (b) JEI Method and Groups=11; (c) JEI Method and Groups=7; (d) JEI-L Method and Groups=15; (e) JEI-L Method and Groups=11; (F) JEI-L Method and Groups=7

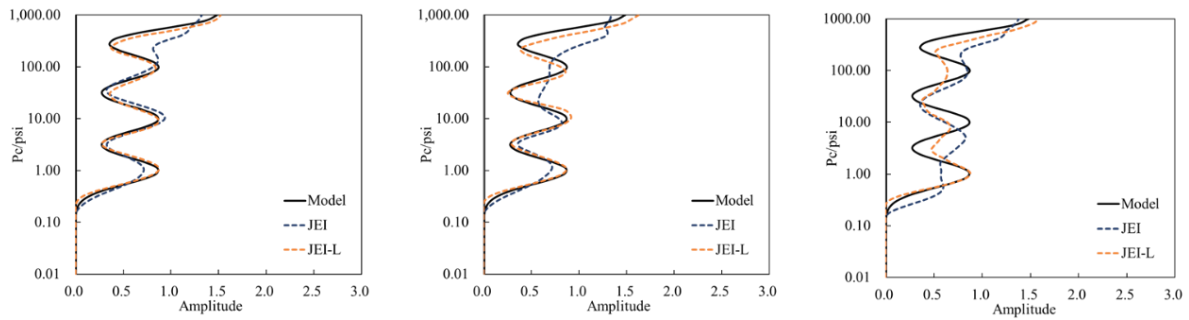


Fig. 8: Pc Components of T2-Pc Map for Different Centrifugal Force Groups. (a) Groups=15; (b) Groups=11; (c) Groups=7

Table 2: Correlation Coefficients (R2) of the Numerical Simulation Results of the Two Methods

Method	Simulation of different SNRs			Simulation of different Groups			Average Correlation Coefficient (R ²)
	SNR=100	SNR=20	SNR=4	Groups =15	Groups= 11	Groups =7	
JEI	0.849	0.836	0.830	0.836	0.744	0.707	0.800
JEI-L	0.980	0.963	0.952	0.963	0.957	0.882	0.950

The numerical simulation results show that the improved joint echo inversion method (JEI-L) can accurately obtain the T2-Pc map, which is suitable for the case of low SNR and a small number of centrifugal force groups. Compared with JEI, the advantages of the improved echo joint inversion method (JEI-L) based on logistic function are mainly reflected in the following aspects.

- (1) In the results obtained by the JEI-L method, the fluid components of different Pc centrifugal forces have better discrimination.
- (2) For the low SNR of T2-Pc core NMR experimental data, the improved JEI-L has better applicability.
- (3) The improved JEI-L method has higher accuracy of inversion results with fewer experimental data in the centrifuge group. Compared with the JEI method, R2 is increased by 0.15, which is closer to 1.

IV. LABORATORY EXPERIMENTAL AND RESULT

A. T2-Pc 2D NMR Experiments

The T2-Pc 2D NMR technique combines the transverse relaxation time (T2) with the capillary pressure (Pc). These two physical quantities need to be obtained through experiments. The steps for conducting core experiments as shown in Fig. 9 are as follows.

Step 1: The standard plunger core samples that have been washed with oil, washed with salt, and dried are treated with pressurized saturated water. Measurement of saturated cores at full water saturation to obtain NMR echo signals.

Step 2: A certain amount of centrifugal force is selected and the core is centrifuged using a high-speed centrifuge. The centrifugal force of the core experiment is the capillary displacement force.

Step 3: Measure the NMR echo signal of the centrifuged core after centrifugation.

Step 4: The centrifuged core is saturated again to obtain a water-saturated core.

Repeat the experiment from step 2 to step 4, and select a different centrifugal force each time when performing step 2.

After the above experimental steps, the NMR echo signals of the cores in the saturated state (the centrifugal force is 0) and the cores after centrifugation with different centrifugal forces were obtained.

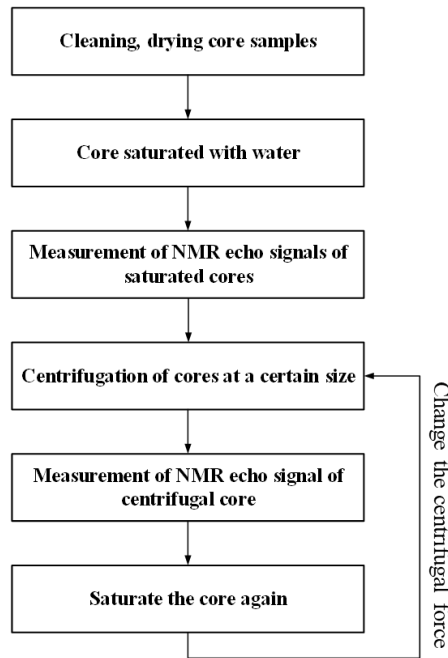


Fig. 9: T2-Pc 2D NMR Experimental Procedure

Four sandstone cores from an area were selected for T2-Pc 2D NMR core experiments. The core information of the experiment is shown in Table 3. According to the method described in the experimental flow of Fig. 9, four cores were subjected to centrifugal experiments with seven different centrifugal forces, and the NMR experiments were carried out. Centrifugal forces are: 0psi, 1.2psi, 4.8psi, 19.1psi, 76.5psi, 172.1psi, 387.3psi. The parameters used for NMR core measurement are as follows: the waiting time (TW) is 4000ms, the echo time (TE) is 0.2ms, the number of echoes is 10000, and the number of superimpositions is 256.

Table 3: Information on Sandstone Cores from an Area

Sample	Porosity/%	Permeability/mD	Bound water saturation/%
1	18.85	5.97	36.13
2	19.83	3.95	37.84
3	8.09	0.195	56.84
4	9.63	0.188	45.98

B. Experimental Results

The T2-Pc core experimental data were processed using the conventional method, JEI, and the modified JEI-L inversion method respectively, and the T2-Pc map results were obtained as shown in Fig. 10 and Fig. 11. In this case, the T2-Pc two-dimensional inversion has 64 steps from 0.1-10000 for T2 and 64 steps from 0.01-1,000 for Pc. The results for T2SDD and DEI show noise signals and negative values in the map of T2SDD. The two-dimensional distribution of the two echo combined inversion methods are relatively close, and both can obtain T2-Pc maps that continuously reflect the pore size and pore throat connectivity of the core.

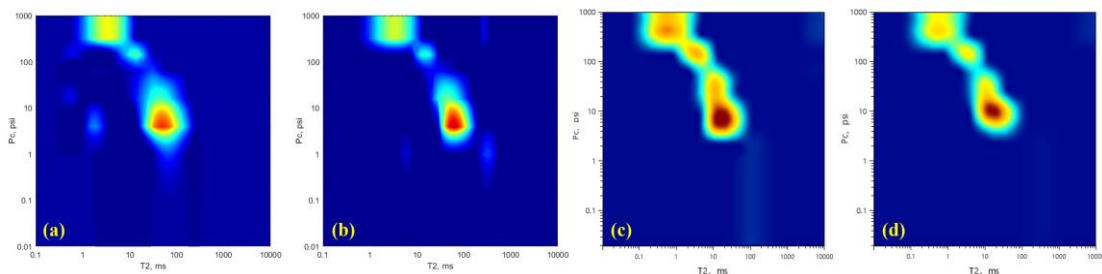


Fig. 10: T2-Pc Map of Sample 1 Obtained by Different Methods. (a) T2SDD; (b) DEI; (c) JEI; (d) JEI-L

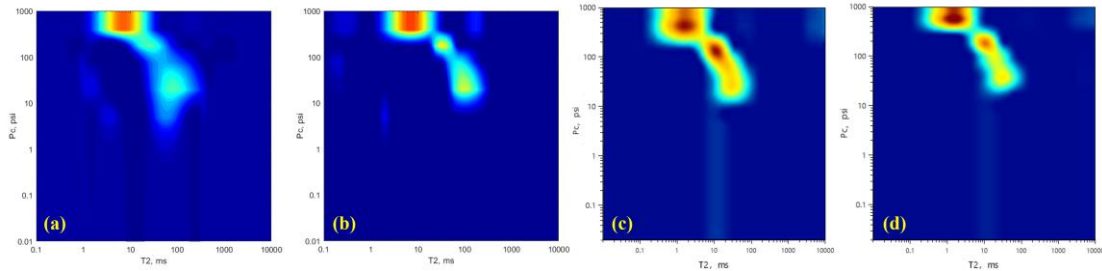


Fig. 11: T2-Pc Maps of Sample 2 Were Obtained by Different Methods. (a) T2SDD; (b) DEI; (c) JEI

The core results show that the improved JEI-L method based on logistic function has a better application effect. The resulting T2-Pc maps are less noisy, more clearly distinguish the different fluid components, and provide a more detailed characterization of the capillary pressure. The results obtained by the JEI-L method are a more realistic representation of the pore throat distribution of the core. In sample 2 shown in Fig. 11, with the increase of the capillary pressure (Pc) value (from 2psi to 50psi), the T2 in the T2-Pc map obtained by the JEI-L method gradually decreases. That is, the radius of the throat decreases, and the pore size decreases correspondingly, reflecting the consistent relationship between the pore and throat. However, when the capillary pressure (Pc) value increases in the T2-Pc map obtained by JEI, the T2 value does not change (T2=44 ms). That is, the radius of the throat decreases while the pore size remains the same. The kernel function (step function) in the JEI algorithm is not continuous, so the T2-Pc result is not completely consistent with the gradual process of the core pore fluid being displaced gradually. The optimized JEI-L method can improve the problem of discontinuous displacement pressure.

C. Characterization of Pore Structure

For rock samples 1 and 3 with significantly different porosity and permeability, the T2 distribution are similar in shape, with the distribution range of 1-200 ms and the similar T2 peak values. It is difficult to characterize the differences between the two core samples only by using the T2 distribution. The T2-Pc 2D map can effectively characterize the distribution of pores and throats in the core, reflecting connectivity. The T2-Pc map of core sample 1 shows significantly better connectivity and permeability than core sample 3. If the same displacement force (100 psi) is used, core sample 1 can displace most of the movable fluid. Similarly, the results of the SEM experiments shown in Fig. 12 indicate a more developed throat and better permeability in sample 1, which is consistent with the characteristics reflected in the T2-Pc maps. Therefore, the T2-Pc map can effectively characterize the pore structure of the cores, conduct an intuitive evaluation of reservoir connectivity, and provide more reservoir information for oil and gas exploration and development, so that we can take corresponding measures to improve oil recovery.

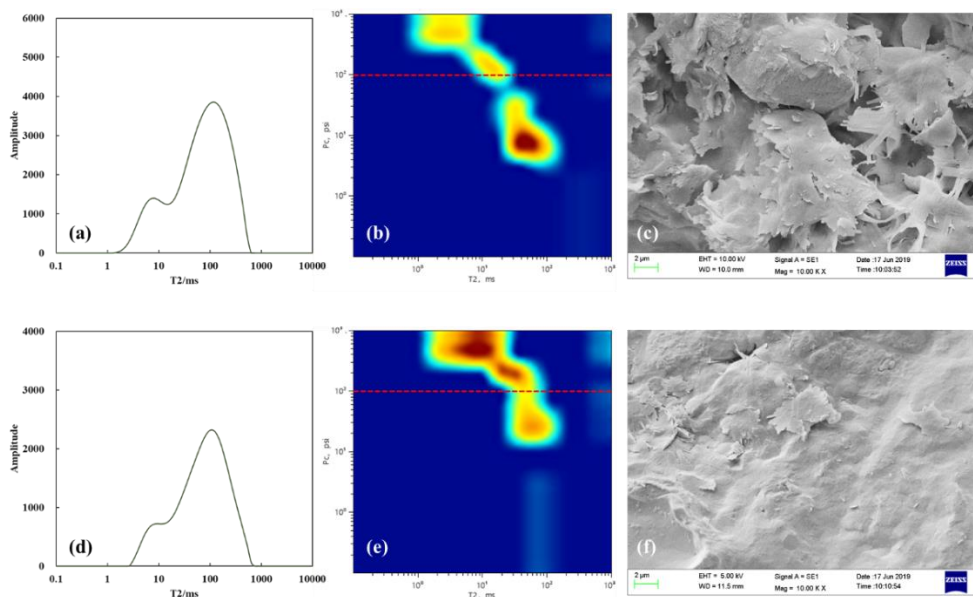


Fig. 12: Results of Core Samples Experiments. (a) T2 Distribution of Sample 1; (b) T2-Pc Map of Sample 1; (c) SEM Results for Rock Sample 1; (d) T2 Distribution of Sample 3; (e) T2-Pc Map of Sample 3; (f) SEM Results for Rock Sample 3

V. CONCLUSION

For T2-Pc 2D NMR experiments, without changing the core measurement experiment process, a joint echo inversion (JEI-L) method is proposed, which uses multiple echo data and is based on the logistic function to obtain the T2-Pc map. The following conclusions are drawn from this study:

(1) Due to the discontinuity of the Heaviside step function, the T2-Pc distribution from the joint echo inversion (JEI) method are not completely consistent with the gradual displacement of the pore fluid in the core. The JEI-L method improved by the logistic continuous function can effectively improve the problem of discontinuous displacement pressure.

(2) Numerical simulations and core experiments show that the advantages of the optimized JEI-L over JEI are more obvious. The capillary pressure (Pc) reflected by the T2-Pc map inversion by JEI-L is more accurate, and the characterization of the pore distribution characteristics of the core is more accurate.

(3) The JEI-L inversion method based on the logistic function is suitable for the case of low SNR and the small number of echo groups with different centrifugal forces. Based on this advantage, the number of centrifugal force groups can be appropriately reduced when conducting T2-Pc 2D NMR core experiments, thereby significantly improving the experimental efficiency.

(4) Although the JEI-L method has made significant progress in T2-Pc 2D NMR experiments, its limitations must be acknowledged. However, the applicability of the method to cores of different lithologies, or even in other porous media materials, is unclear.

(5) The research on the improvement of the inversion method shows that in the multi-dimensional and multi-physics correlation distribution research, it is very important to accurately describe the laws of non-MR physical quantities. In the future, we may be able to express the kernel function of the physical processes of fluid changes in porous media when physical quantities such as temperature and pressure are changed, forming the NMR-X technique, where X represents the information of any non-NMR physical quantities, and thus establishing a close connection of multidimensional multi-physical quantities, reflecting the effect of the coupling relationship between different physical quantities on the results of the hydrogen kernel measurements.

ACKNOWLEDGMENT

We would like to thank Harry Xie and Yuanyuan Luo for the constructive suggestions that significantly improved the manuscript.

REFERENCES

- [1] Coates, G., Xiao, L., Prammer, M., 2000. NMR logging principles and applications, Houston: Gulf Publishing Company, USA.
- [2] Dunn, K.J., Bergman, J., Latorraca, A., 2002. Nuclear magnetic resonance petrophysical and logging application, Handbook of Geophysical Exploration. Pergamon, New York.
- [3] Song, Y.-Q., 2013. Magnetic resonance of porous media (MRPM): A perspective. *Journal of Magnetic Resonance*, 229: 12-24.
- [4] Dick, Michael J., Veselinovic, Dragan, and Derrick Green. Review of Recent Developments in NMR Core Analysis. *Petrophysics* 63 (2022): 454–484.
- [5] Yao, Y., Liu, D., Che, Y. et al., 2010. Petrophysical characterization of coals by low-field nuclear magnetic resonance (NMR). *Fuel*, 89(7): 1371-1380.
- [6] Zhang, P., Lu, S., Li, J. et al., 2018. Petrophysical characterization of oil-bearing shales by low-field nuclear magnetic resonance (NMR). *Marine and Petroleum Geology*, 89: 775-785.
- [7] Song, Y.-Q., Kausik, R., 2019. NMR application in unconventional shale reservoirs – A new porous media research frontier. *Progress in Nuclear Magnetic Resonance Spectroscopy*, 112-113: 17-33.
- [8] Stapf, S., Shikhov, I., Arns, C., et al. 2023. Dipolar NMR relaxation of adsorbates on surfaces of controlled wettability. *Magnetic Resonance Letters*, 3(3), 220-231.
- [9] Zheng, S., Yao, Y., Liu, D. et al., 2018. Characterizations of full-scale pore size distribution, porosity and permeability of coals: A novel methodology by nuclear magnetic resonance and fractal analysis theory. *International Journal of Coal Geology*, 196: 148-158.
- [10] Rylander, E., Philip, M.S., Jiang, T. et al., 2013. NMR T2 distributions in the eagle ford shale: Reflections on pore size, SPE Unconventional Resources Conference-USA, pp. 10-12.
- [11] Testamanti, M.N., Rezaee, R., 2017. Determination of NMR T2 cut-off for clay bound water in shales: A case study of Carynginia Formation, Perth Basin, Western Australia. *Journal of Petroleum Science and Engineering*, 149: 497-503.
- [12] Huang, X., Li, T., Wang, X. et al., 2019. Distribution characteristics and its influence factors of movable fluid in tight sandstone reservoir: a case study from Chang-8 oil layer of Yanchang Formation in Jiyuan oilfield, Ordos Basin. *Acta Petrolei Sinica*, 40(5): 557-567.

- [13] Li, H., Guo, H., Li, H. et al., 2015. Thickness analysis of bound water film in tight reservoir. *Natural Gas Geoscience*, 26(1): 186-192.
- [14] Wang, X., Fan, Y., Deng, S.u. et al., 2009. Irreducible water saturation determination based on centrifugal test data. *Journal of China University of Petroleum (Edition of Natural Science)* 33(3): 76-79.
- [15] Li, T., Guo, H., Li, H. et al., 2013. Experimental research on movable fluid and NMR T2cutoff in tight sandstone. *Science Technology and Engineering*, 13(3): 701-704.
- [16] Li, Z., Liu, W., Sun, D. et al., 2011. Experimental study on T2 cutoff value of the movable fluid in high-porosity low-permeability carbonate rock. *Journal of Xi'an Shiyou University (Natural Science Edition)*, 26(5): 76-79.
- [17] Lyu, C., Ning, Z., Cole, D.R. et al., 2020. Experimental investigation on T2 cutoffs of tight sandstones: Comparisons between outcrop and reservoir cores. *Journal of Petroleum Science and Engineering*, 191: 107184.
- [18] Lyu, C., Ning, Z., Wang, Q. et al., 2018. Application of NMR T2 to pore size distribution and movable fluid distribution in tight sandstones. *Energy & Fuels*, 32.
- [19] Zhou, S., Liu, H., Yan, G. et al., 2016. NMR research of movable fluid and T2 cutoff of marine shale in South China. *Oil & Gas Geology*, 37(4): 612-616.
- [20] Lei, Q., Cheng, L., Wang, C. et al., 2017. A study on distribution features of movable fluids for Chang 7 tight reservoir in Ordos Basin. *Natural Gas Geoscience*, 28(1): 26-31.
- [21] Zhang, S., Wang, J., Zhang, Y. et al., 2021. Determination of petrophysical property cutoffs of lacustrine dolomite intercrystalline pore reservoir in the Xiaganchaigou Formation, western Q aidam Basin. *Acta Petrolei Sinica*, 42(1): 45-55,118.
- [22] Jiang, Y., Xu, G., Bi, H. et al., 2021. A new method to determine surface relaxivity of tight sandstone cores based on LF-NMR and high-speed centrifugation measurements. *Journal of Petroleum Science and Engineering*, 196: 108096.
- [23] Li, R., Shikhov, I., Arns. C. H. Bayesian optimization with transfer learning: A study on spatial variability of rock properties using NMR relaxometry. *Water Resources Research*, 2022, 58(9): e2021WR031590.
- [24] Elsayed, M., Al-Abdrabalnabi, R., Zhou, X. et al., 2022. Influence of long-term stored oil on wettability and its recovery in depleted petroleum reservoirs. *Energy Reports*, 8: 2085-2099.
- [25] Shoukry, Aktham E., Saraji, et al. Pore-scale experimental investigation of capillary desaturation in fractured porous media. *Journal of Hydrology*, 2024, 631: 130748.
- [26] Xu, W., Huang, H., Ke, S. et al., 2022. An integral method for calculation of capillary pressure based on centrifuge data of tight sandstone. *Petroleum Science*, 19(1): 91-99.
- [27] Chen, Y., Zhang, G., Zheng, G. et al., 2021. Core testing technology with T2-Pc two-dimensional nuclear magnetic resonance and its application. *Petroleum Geology & Experiment*, 43(3): 549-556.
- [28] Bratland, A.M.L., Seland, J.G., 2021. Multidimensional dynamic NMR correlations in sedimentary rock cores at different liquid saturations. *Journal of Magnetic Resonance*, 327: 106963.
- [29] Fan, Y., Wu, F., Li, H. et al., 2015. A modified design of pulse sequence and inversion method for D-T2 two-dimensional NMR. *Acta Physica Sinica*, 64(9).
- [30] Hürliemann, M.D., Venkataramanan, L., 2002. Quantitative measurement of two-dimensional distribution functions of diffusion and relaxation in grossly inhomogeneous fields. *Journal of Magnetic Resonance*, 157(1): 31-42.
- [31] Yang, C., Chen, J., Zeng, Q. et al., 2022. Simultaneous acquirement of pure shift 2D homonuclear correlation distribution. *Journal of Magnetic Resonance*, 339: 107229.
- [32] Song, Y.-Q., Souza, A., Vembusubramanian, M. et al., 2021. Multiphysics NMR correlation spectroscopy. *Journal of Magnetic Resonance*, 322: 106887.
- [33] Deng, L., Guo, W., Huang, T., 2016. Single image super-resolution by approximated Heaviside functions. *Information Sciences*, 348: 107-123.
- [34] Wang, Z., Timlin, D., Kouznetsov, M. et al., 2020. Coupled model of surface runoff and surface-subsurface water movement. *Advances in Water Resources*, 137: 103499.
- [35] Bulgarelli, N.A.V., Biazussi, J.L., Monte Verde, W. et al., 2021. Experimental investigation on the performance of Electrical Submersible Pump (ESP) operating with unstable water/oil emulsions. *Journal of Petroleum Science and Engineering*, 197: 107900.
- [36] Gallagher, B., 2011. Peak oil analyzed with a logistic function and idealized Hubbert curve. *Energy Policy*, 39(2): 790-802.
- [37] Saravanan, Rajendran, Chakraborty, et al. Exact diffusion dynamics of a Gaussian distribution in one-dimensional two-state system. *Chemical Physics Letters*, 2019, 731: 136567.